ACS Medicinal Chemistry Letters

Letter

pubs.acs.org/acsmedchemlett

Factors Influencing *in Vivo* Disposition of Polymeric Micelles on Multiple Administrations

Eri Hara,[†] Motoki Ueda,[‡] Akira Makino,[§] Isao Hara,[∥] Eiichi Ozeki,[∥] and Shunsaku Kimura*[,⊥]

[†]Department of Experimental Therapeutics, Institute for Advancement of Clinical and Translational Science, Kyoto University Hospital, 53 Shogoin-kawahara-cho, Sakyo-ku, Kyoto 606-8507, Japan

[‡]Clinical Division of Diagnostic Radiology, Kyoto University Hospital, 53 Shogoin-kawahara-cho, Sakyo-ku, Kyoto 606-8507, Japan

[§]Division of Molecular Imaging, Biomedical Imaging Research Center, University of Fukui, 23-3 Matsuokashimoaizuki, Eiheiji-cho, Yoshida-gun, Fukui 910-1193, Japan

[∥]Technology Research Laboratory, Shimadzu Corporation, 3-9-4 Hikari-dai, Seika-cho, Soraku-gun, Kyoto 619-0237, Japan

[⊥]Department of Material Chemistry, Graduate School of Engineering, Kyoto University, Kyoto daigaku-katsura, Nishikyo-ku, Kyoto 615-8510, Japan

Supporting Information

ABSTRACT: Lactosome is a polymeric micelle composed of amphiphilic polydepsipeptide, poly(sarcosine)$_{64}$-*block*-poly(L-lactic acid)$_{30}$ (AB-type), which accumulates in solid tumors through the enhanced permeability and retention (EPR) effect. However, lactosome on multiple administrations changed its pharmacokinetics from accumulation in tumors to liver due to the production of antilactosome IgM, which was triggered by the first administration. This phenomenon is called the accelerated blood clearance (ABC). In order to reduce the production of antilactosome IgM, a novel nanoparticle composed of (poly(sarcosine)$_{23}$)$_3$-*block*-poly(L-lactic acid)$_{30}$ (A_3B-type) was prepared. The A_3B-type lactosome at the second administration showed an *in vivo* disposition similar to that at the first administration due to suppression of antibody production. This study involving the AB- and A_3B-type lactosomes, with variation of conditions, revealed that the high local density of poly(sarcosine) chains of the A_3B-type lactosome should relate to the prevention of a polymeric micelle from interacting B-cell receptors.

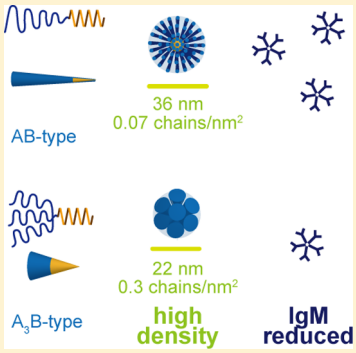

KEYWORDS: *Molecular imaging, nanoparticle, ABC phenomenon, IgM, pharmacokinetics, block polymer*

Nanoparticles of polymeric micelles have high potential for tumor imaging and antitumor therapy.[1,2] These micelles accumulate in solid tumors through the enhanced permeability and retention (EPR) effect of high permeability across blood vessels and immature lymphatic drain systems.[3,4] Indeed, polymeric micelles loaded with antitumor drugs have been widely studied for clinical applications.[5]

Lactosome is a polymeric micelle, which is composed of amphiphilic polydepsipeptide with a hydrophilic poly(sarcosine) block and a hydrophobic poly(L-lactic acid) block (AB-type).[6] The amphiphilic polydepsipeptide is biodegradable and biocompatible.[7,8] Further, lactosome is hardly recognized by the mononuclear phagocyte system (MPS) leading to a long lifetime in the bloodstream. On the basis of the long *in vivo* blood clearance time, the near-infrared fluorescent probe (NIRF)-labeled lactosome was successful for imaging of various solid tumors. Especially, the orthotopic liver tumor was clearly imaged due to the low background of the healthy liver region showing highly selective accumulation of lactosome in tumors.[9] Lactosome has been studied as a nanocarrier of probes for positron emission tomography (PET) imaging,[10] tumor targeting,[11] and intraoperative imaging.[12]

However, the AB-type lactosome has a drawback of alteration of *in vivo* disposition on multiple administrations.[13] At the first administration, the AB-type lactosome showed a long lifetime in the bloodstream, but at the second administration, the AB-type lactosome accumulated immediately in liver, resulting in the rapid clearance from the bloodstream. The similar effect has been already reported with PEGylated liposome and named as the accelerated blood clearance (ABC) phenomenon.[14−16] The ABC phenomenon was reported with another polymeric micelle using PEG as a hydrophilic block.[17] It is therefore suggested that the ABC phenomenon may be commonly observed with nanoparticles. This phenomenon has been clarified due to the production of antinanoparticle IgM upon the first administration of nanoparticle. The hydrophilic polymer chains surrounding the nanoparticles are found to be T-independent antigens to induce the immune reaction.[16] In the case of lactosome, poly(sarcosine) covering the surface was identified as an antigen by the competitive inhibition assay.[13]

Received: March 16, 2014
Accepted: June 18, 2014
Published: June 18, 2014

 © 2014 American Chemical Society dx.doi.org/10.1021/ml500112u | *ACS Med. Chem. Lett.* 2014, 5, 873−877

In order to suppress the immune reaction against nanoparticles, there have been several reports that were recently reviewed by Ishida et al.[18] So far, factors of nanoparticle size, different kinds of hydrophilic chains and core structure of the core−shell micelle, and the administration regimen have been discussed.[19,20] We are here to discuss another factor, that of the surface density of the hydrophilic polymer chains on the polymeric micelle. This study is in the same line of the surface modification with polymer brushes in the field of polymer materials.[21,22] When the surface modifying polymer chains become a high-density polymer brush state corresponding to a surface density of 0.3 chains/nm^2 or over, the surface shows a lubricating surface and also an antifouling property, etc. We designed a novel amphiphilic polydepsipeptide having three hydrophilic branch chains connected to one hydrophobic poly(lactic acid) chain (A_3B-type). The A_3B-type polymeric micelle size went down to ca. 22 nm from the AB-type of ca. 36 nm.[23] However, the *in vivo* clearance time of the A_3B-type lactosome became shorter than that of the AB-type lactosome, which factor was taken into consideration later (Table 1).

Table 1. Characterizations of the AB- and A_3B-Type Lactotomes

type	hydrodynamic diameter (nm)[a]	PDI	poly(Sar) density (chain/nm^2)[b]	blood half-time (h)[c]
AB	36.0 ± 0.5	0.05	0.07	17.2
A_3B	22.3 ± 0.3	0.05	0.30	4.3

[a]The data obtained by DLS measurement (n = 3). [b]The details are shown in Supplemental Table S1. [c]The decays of the lactosomes in the bloodstream are shown in Supplemental Figure S1.

Further, we found that the hydrodynamic diameters of these lactosomes can be precisely adjustable with loading benzyloxycarbonyl-poly(L-lactic acid)$_{30}$ (Z-PLLA$_{30}$). Therefore, we could prepare the AB- and A_3B-type lactosomes having the same hydrodynamic diameter, which enabled us to evaluate separately the two factors of the nanoparticle size and the surface density of the poly(sarcosine) chains influencing the ABC phenomenon.

The AB-type lactosome is composed of poly(sarcosine)$_{64}$-*block*-poly(L-lactic acid)$_{30}$, and the hydrodynamic diameter was ca. 36 nm (Figure 1A,C). However, the A_3B-type lactosome prepared from (poly(sarcosine)$_{23}$)$_3$-*block*-poly(L-lactic acid)$_{30}$ shows a smaller hydrodynamic diameter of ca. 22 nm (Figure 1B,D). Transmission electron microscopy (TEM) images also showed the spherical polymeric micelles of the AB- and A_3B-type polymers having diameters of ca. 34 and 21 nm, respectively.[23] The magnified views are shown in Supplemental Figure S2. Accordingly, the surface density of poly(sarcosine) chains on the A_3B-type lactosome became 4 times higher than that on the AB-type lactosome (Table 1). However, the half-lifetime in the bloodstream of the A_3B-type lactosome was found to be 4.3 h, which was much shorter than the AB-type lactosome of 17.2 h. The data suggest that the *in vivo* stability of the A_3B-type lactosome was impaired probably by accommodating so many hydrophilic chains into the shell layer of the polymeric micelle. The critical association concentrations (CAC) of the AB- and A_3B-type lactosomes were found to be as low as 1.3×10^{-8} and 1.9×10^{-9} M, respectively (on the basis of the general evaluation method using a fluorescent probe of pyrene (Supplemental Figure S3)). Although the *in vivo* stability of the A_3B-type lactosome was impaired, the self-assembling propensity remains high.

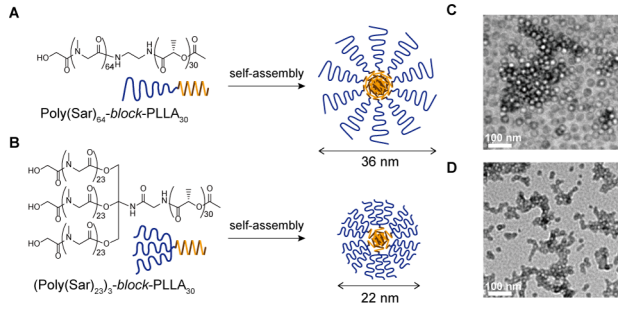

Figure 1. Schematic presentation of the AB- and A_3B-type polymeric micelles (A,B). TEM images of the AB- and A_3B-type micelles (C,D).

Production of antilactosome IgM at 7 days after the AB- or A_3B-type lactosome administration was evaluated by ELISA (Figure 2A). The production of antilactosome IgM was lower

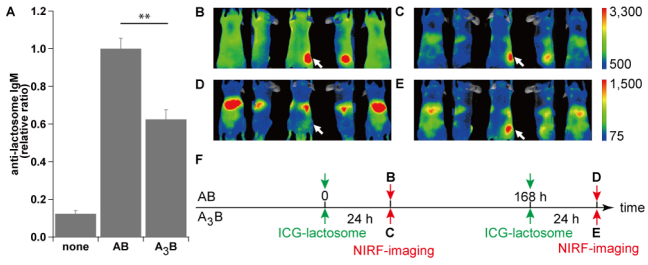

Figure 2. IgM productions upon the administrations of the AB- and A_3B-type lactosomes (A) (n = 3 per group). Antilactosome IgM productions are normalized by taking the antilactosome IgM production with the AB-type lactosome as a reference, 1.0. Pharmacokinetic changes (NIRF images) upon multiple doses of the AB- (B,D) and A_3B-type (C,E) lactosomes. The images D and E were taken at 7 days after the first administration of the AB- and A_3B-type lactosomes. The time schedule is shown in panel F.

with the A_3B-type lactosome than the AB-type lactosome, indicating the lower immunogenicity of the A_3B-type lactosome than the AB-type lactosome.

In vivo dispositions of the lactosomes were analyzed by NIRF imaging. The AB-type lactosome at the first administration spread over the whole body and gradually accumulated in the tumor region due to the EPR effect (Figure 2B). However, the AB-type lactosome on the second administration at 7 days after the first administration accumulated immediately in liver as previously reported (Figure 2D).[13] However, the A_3B-type lactosome spread over the whole body to accumulate in the tumor region at either the first or the second administration (Figure 2C,E).

Region-of-interest (ROI) analyses also support that the accumulation amount of the A_3B-type lactosome in the tumor region (the right femoral region, Figure 2E) was 3−5 times higher than that at the healthy left femoral region at the second administration (Figure 3A). The accumulation ratios of liver against background by ROI analyses also show that the liver accumulation of the A_3B-type lactosome was significantly low just after the second administration followed by a moderate increase, while the AB-type lactosome accumulated strongly in liver even right after the second administration (Figure 3B).

The AB- and A_3B-type lactosomes showed the different life times in the bloodstream. In order to look into the effect of this difference on the ABC phenomenon, we maintained the

dx.doi.org/10.1021/ml500112u | ACS Med. Chem. Lett. 2014, 5, 873−877

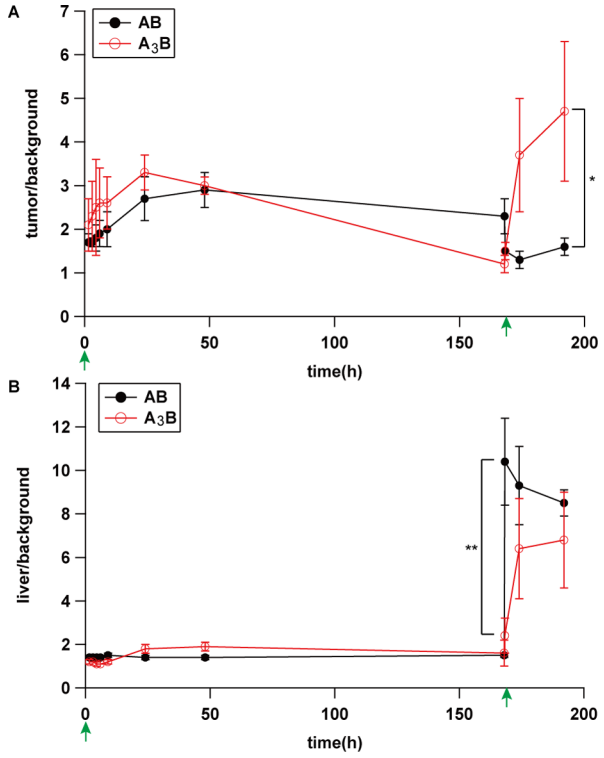

Figure 3. Time profiles of the ratio of ROI at tumor against background (tumor/background) (A). Time profiles of the ratio of ROI at liver against background (liver/background) (B). The *p* value: not significant (NS), $*p < 0.05$, $**p < 0.01$.

concentration of the A_3B-type lactosome in blood by the repeated administrations at 4 h intervals (0, 4, and 8 h). With the repeated administrations, the concentration in blood was kept high (Figure 4A), but the production of antilactosome IgM was found to remain as low as the single administration of the A_3B-type lactosome (Figure 4B).

The nanoparticle size of the lactosomes can be increased by loading Z-$PLLA_{30}$ in the hydrophobic core of the polymeric micelle.[23] The A_3B-type lactosome increased the hydrodynamic diameter gradually with loading Z-$PLLA_{30}$ up to 39 nm from 22

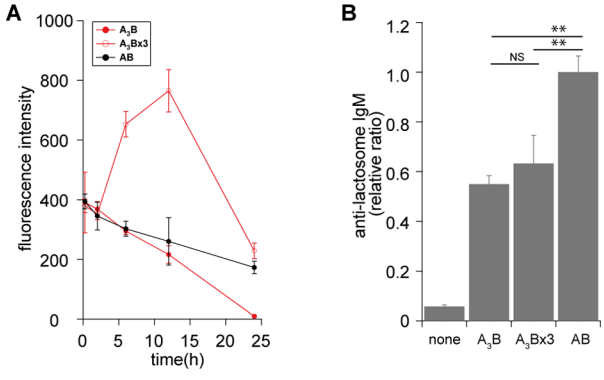

Figure 4. Time profiles of lactosome concentrations in blood using ICG-labeled AB- and A_3B-type lactosomes (A). Productions of the antilactosome IgM with the single dose, the triplicate doses of the A_3B-type lactosome, and the single dose of the AB-type lactosome (B). Antilactosome IgM productions are normalized by taking that with the AB-type lactosome as 1.0. A_3Bx3 represents the triplecate doses of the A_3B-type lactosome at 4 h intervals.

nm (PDI = 0.038−0.070) (Figure 5A). Similarly, the AB-type lactosome is variable in size from 38 to 52 nm (PDI = 0.052−

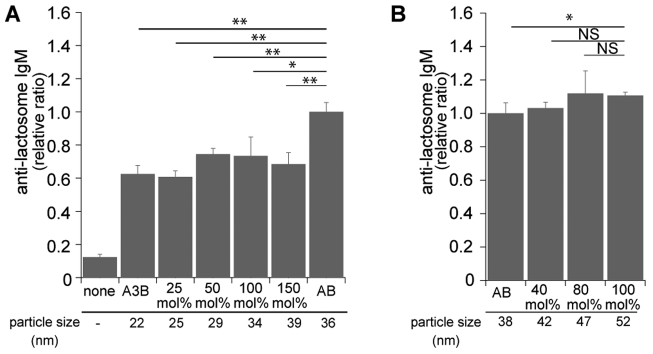

Figure 5. Productions of antilactosome IgM with lactosomes varying the particle sizes. The A_3B-type lactosomes increased the size from 22 to 39 nm with the addition of Z-$PLLA_{30}$ from 0 mol % to 150 mol % (A). The AB-type lactosomes increased the size from 38 to 52 nm with the addition of Z-$PLLA_{30}$ from 0 mol % to 100 mol % (B). Antilactosome IgM productions are normalized by taking that with the AB-type lactosome as 1.0. The *p* value: not significant (NS), $*p < 0.05$, $**p < 0.01$.

0.123) with loading Z-$PLLA_{30}$ (Figure 5B). Productions of antilactosome IgM were evaluated by ELISA with using these lactosomes of different nanosizes (Figure 5A,B). It is clearly shown that the anti-A_3B-type lactosome IgM productions were lower than the anti-AB-type lactosome IgM productions (Figure 5A). However, the size dependences of the antilactosome IgM productions were not obvious within the each group of the A_3B- and AB-type lactosomes (Figure 5A,B).

However, a difference of antilactosome IgM productions between two groups of the A_3B- and AB-type lactosomes was significant in the whole range of the micelle sizes examined here (Figure 6). Notably, when the antilactosome IgM amounts were compared between the A_3B- and AB-type lactosomes of the similar size of ca. 40 nm, the former became lower than the

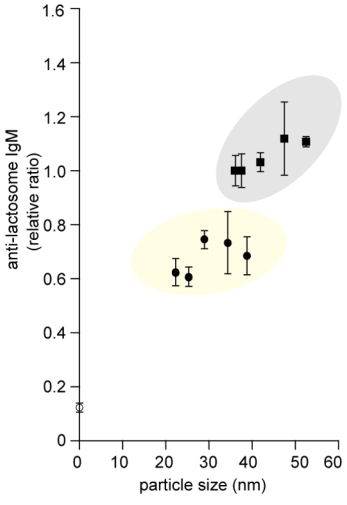

Figure 6. Size dependences of antilactosome IgM productions with administrations of the AB- and A_3B-type lactosomes. The graph is reconstructed from data of Figure 5. Antilactosome IgM productions are normalized by taking that with the AB-type lactosome as 1.0 ($n = 3$ per group).

dx.doi.org/10.1021/ml500112u | ACS Med. Chem. Lett. 2014, 5, 873−877

latter, suggesting that the size of the polymeric micelle should not be critical for the antilactosome IgM production.

In regard to the ABC phenomenon of the AB-type lactosome, the level of antilactosome IgM started to increase from 3 days after the first administration up to a saturation level at 5 days and later.[13] The AB-type lactosome on the following administration at later than 5 days from the first administration accumulated immediately in liver due to the recognition by antilactosome IgM, which was confirmed by NIRF imaging using the NIRF-labeled lactosome. In the present study, we have evaluated the A_3B-type lactosome on the ABC phenomenon. The A_3B-type lactosome is composed of the same hydrophilic and hydrophobic blocks as the AB-type lactosome, but the hydrophilic block number in one molecule of the A_3B-type lactosome is three times higher than the AB-type lactosome, which raises the local density of poly(sarcosine) chains on the surface. Notably, the A_3B-type lactosome attenuated the ABC phenomenon compared with the AB-type lactosome as shown by NIRF imaging and the antilactosome IgM production.

As far as the attenuation of the ABC phenomenon is concerned, there have been already several reports; (1) the PEGylated polymeric micelles decreasing the particle size to less than 30 nm,[24] (2) coating of nanoparticles with poly(*N*-vinyl-2-pyrrolidone),[25] (3) modification of liposome surface with a polyglycerol-derived lipid,[18] (4) a PEG-shell-possessing polymeric micelle with a hydrophilic inner core (PEG-P(Lys-DOTA-Gd),[26] and (5) alteration of the administration regimen of using high doses and the prolongation of a time interval between injections.[18] Actually, the A_3B-type lactosome with a 22 nm diameter attenuated the ABC phenomenon, which may be categorized into group (1) described above. However, there are some controversies here against the interpretation that the particle size is crucial for the ABC phenomenon. The A_3B-type lactosome with loading Z-$PLLA_{30}$ to increase the particle size up to 40 nm still showed the suppression effect on the antilactosome IgM production as much as the A_3B-type lactosome of 22 nm (Figure 5A). Even though these lactosomes have the similar particle size of 40 nm, the A_3B-type lactosome significantly suppressed the antilactosome IgM production compared with the AB-type lactosome (Figure 6). Small particle size should be favorable for suppression of the antilactosome IgM production, but the size is not simply all the trigger for the ABC phenomenon.

We can now raise two factors for the ABC phenomenon. One is the blood clearance time and the other is the local density defined by the micelle size, the chain length of the hydrophilic blocks, and the molecular shape. The half-lifetime in the bloodstream of the A_3B-type lactosome was 4.3 h, which is considerably shorter than the AB-type lactosome of 17.2 h (Table 1). The shorter lifetime of nanoparticles should result in less chance to trigger the immune system. Indeed, Ishihara et al. reported that the ABC phenomenon was not induced upon the repeated injections of the PVP-coated nanoparticles, which have a short lifetime in the bloodstream.[25] Here, the triplicate doses of the A_3B-type lactosome at 4 h intervals with keeping the high concentration in blood did not increase the IgM production from that with the single dose. The shorter half-time is therefore not the major factor for the reduction of the ABC phenomenon (Figure 4).

The surface density of the hydrophilic blocks differs significantly between the two kinds of lactosomes. The surface density reaches to 0.30 chain/nm^2 for the A_3B-type lactosome, which is 4 times higher than 0.07 chain/nm^2 for the AB-type lactosome (Table 1). Even though the high surface density should decrease with incorporation of Z-$PLLA_{30}$ into the A_3B-type lactosomes, the three poly(sarcosine) chains are bundled at the C-terminal resulting in locally a high density of poly(sarcosine) chains (the molecular shape effect). However, in the case of the AB-type micelle, a long poly(sarcosine) block of 64-mer should generate a loose space at the peripheral region of the shell layer of the polymeric micelle. The short poly(sarcosine) blocks of 23-mer employed for the A_3B-type lactosome might be another reason for raising the local high density of poly(sarcosine) chains because the shorter chains can avoid the curvature effect.

Then, we currently have been trying to study the chain length effect on the ABC phenomenon. Two other A_3B-type lactosomes having longer poly(sarcosine) chains of 33-mer and 50-mer were prepared. These A_3B-type lactosomes also formed polymeric micelles with a diameter less than 30 nm. Interestingly, these lactosomes did not show the ABC phenomenon either because the *in vivo* imaging showed that the liver capture right after the second administration was not significant (Supplemental Figure S4). Further, a long poly(sarcosine) block of 60-mer did not induce the ABC phenomenon when the poly(sarcosine) block was expressed densely at the surface of peptide-nanosheets prepared by self-assembling of an amphiphilic polypeptide, poly(sarcosine)$_{60}$-*block*-(L-Leu-Aib)$_6$.[27] All these results support the interpretation that the high local density of poly(sarcosine) chains rather than the poly(sarcosine) chain length should be a major cause for suppression of the ABC phenomenon. It is considered that the locally packed poly(sarcosine) chains may exclude other molecules from penetration into the surface region and prevent the polymeric micelle from interacting with B-cell receptors.

One drawback of the A_3B-type lactosome is, however, the decrease of the tumor accumulation due to the shorter lifetime in the bloodstream (Supplemental Figure S5). We are now finding out the optimal chain length of poly(sarcosine) and composition of lactosome to stabilize the polymeric micelle structure to improve the accumulation in tumor with the attenuated ABC phenomenon.

Applications of nanoparticles for diagnosis and therapy are currently appealing. However, the ABC phenomenon with nanoparticles should be solved out before putting the nanoparticles on clinical researches. So far, there have been several ways reported to attenuate the ABC phenomenon, but the detailed mechanism remains to be solved. Here, the local density of poly(sarcosine) chains of lactosomes was shown to influence the ABC phenomenon. We think that the higher local density of the surrounding hydrophilic polymer chains should be related with prevention of the interaction between micelles and B cell receptors, but further studies are needed to make it clear.

■ ASSOCIATED CONTENT

Supporting Information

Experimental procedures and supporting results. This material is available free of charge via the Internet at http://pubs.acs.org.

■ AUTHOR INFORMATION

Corresponding Author

*(S.K.) Phone: +81-75-383-2400. Fax: +81-75-383-2401. E-mail: shun@scl.kyoto-u.ac.jp.

Funding

This study is a part of joint research, which is focusing on the development of the basis of technology for establishing COE for nanomedicine, carried out through Kyoto City Collaboration of Regional Entities for Advancing Technology Excellence (CREATE), Japan Science and Technology Agency, a part of the project entitled "Development of PET Probe for Imaging Solid Tumors Using Nanocarriers" under the contract of Innovation plaza Kyoto, Japan Science and Technology Agency, and a part of the Innovative Techno-Hub for Integrated Medical Bio-Imaging of the Project for Developing Innovation Systems, from the Ministry of Education, Culture, Sports, Science and Technology (MEXT).

Notes

The authors declare no competing financial interest.

■ ACKNOWLEDGMENTS

We thank Dr. M. Sugai (Department of Experimental Therapeutics, Institute for Advancement of Clinical and Translational Science, Kyoto University Hospital) for discussion.

■ REFERENCES

(1) Cabral, H.; Matsumoto, Y.; Mizuno, K.; Chen, Q.; Murakami, M.; Kimura, M.; Terada, Y.; Kano, M. R.; Miyazono, K.; Uesaka, M.; Nishiyama, N.; Kataoka, K. Accumulation of sub-100 nm polymeric micelles in poorly permeable tumours depends on size. *Nat. Nanotechnol.* **2011**, *6*, 815−823.

(2) Lukyanov, A. N.; Hartner, W. C.; Torchilin, V. P. Increased accumulation of PEG-PE micelles in the area of experimental myocardial infarction in rabbits. *J. Controlled Release* **2004**, *94*, 187−193.

(3) Fang, J.; Nakamura, H.; Maeda, H. The EPR effect: Unique features of tumor blood vessels for drug delivery, factors involved, and limitations and augmentation of the effect. *Adv. Drug Delivery Rev.* **2011**, *63*, 136−151.

(4) Matsumura, Y.; Maeda, H. A new concept for macromolecular therapeutics in cancer-chemotherapy: mechanism of tumoritropic accumulation of proteins and the antitumor agent smancs. *Cancer Res.* **1986**, *46*, 6387−6392.

(5) Croy, S. R.; Kwon, G. S. Polymeric micelles for drug delivery. *Curr. Pharm. Des.* **2006**, *12*, 4669−4684.

(6) Makino, A.; Yamahara, R.; Ozeki, E.; Kimura, S. Preparation of novel polymer assemblies, "lactosome", composed of poly(L-lactic acid) and poly(sarcosine). *Chem. Lett.* **2007**, *36*, 1220−1221.

(7) Eschenbrenner, M.; Jorns, M. S. Cloning and mapping of the cDNA for human sarcosine dehydrogenase, a flavoenzyme defective in patients with sarcosinemia. *Genomics* **1999**, *59*, 300−308.

(8) Nampoothiri, K. M.; Nair, N. R.; John, R. P. An overview of the recent developments in polylactide (PLA) research. *Bioresour. Technol.* **2010**, *101*, 8493−8501.

(9) Makino, A.; Kizaka-Kondoh, S.; Yamahara, R.; Hara, I.; Kanzaki, T.; Ozeki, E.; Hiraoka, M.; Kimura, S. Near-infrared fluorescence tumor imaging using nanocarrier composed of poly(L-lactic acid)-*block*-poly(sarcosine) amphiphilic polydepsipeptide. *Biomaterials* **2009**, *30*, 5156−5160.

(10) Yamamoto, F.; Yamahara, R.; Makino, A.; Kurihara, K.; Tsukada, H.; Hara, E.; Hara, I.; Kizaka-Kondoh, S.; Ohkubo, Y.; Ozeki, E.; Kimura, S. Radiosynthesis and initial evaluation of f-18 labeled nanocarrier composed of poly(L-lactic acid)-*block*-poly(sarcosine) amphiphilic polydepsipeptide. *Nucl. Med. Biol.* **2013**, *40*, 387−394.

(11) Hara, E.; Makino, A.; Kurihara, K.; Ueda, M.; Hara, I.; Kawabe, T.; Yamamoto, F.; Ozeki, E.; Togashi, K.; Kimura, S. Radionuclide therapy using nanoparticle of I-131-lactosome in combination with percutaneous ethanol injection therapy. *J. Nanopart. Res.* **2013**, *15*, 2131.

(12) Funayama, T.; Sakane, M.; Abe, T.; Hara, I.; Ozeki, E.; Ochiai, N. Intraoperative near-infrared fluorescence imaging with novel indocyanine green-loaded nanocarrier for spinal metastasis: A preliminary animal study. *Open Biomed. Eng. J.* **2012**, *6*, 80−84.

(13) Hara, E.; Makino, A.; Kurihara, K.; Yamamoto, F.; Ozeki, E.; Kimura, S. Pharmacokinetic change of nanoparticulate formulation "lactosome" on multiple administrations. *Int. Immunopharmacol.* **2012**, *14*, 261−266.

(14) Dams, E. T. M.; Laverman, P.; Oyen, W. J. G.; Storm, G.; Scherphof, G. L.; Van der Meer, J. W. M.; Corstens, F. H. M.; Boerman, O. C. Accelerated blood clearance and altered biodistribution of repeated injections of sterically stabilized liposomes. *J. Pharmacol. Exp. Ther.* **2000**, *292*, 1071−1079.

(15) Ishida, T.; Maeda, R.; Ichihara, M.; Irimura, K.; Kiwada, H. Accelerated clearance of PEGylated liposomes in rats after repeated injections. *J. Controlled Release* **2003**, *88*, 35−42.

(16) Koide, H.; Asai, T.; Hatanaka, K.; Akai, S.; Ishii, T.; Kenjo, E.; Ishida, T.; Kiwada, H.; Tsukada, H.; Oku, N. T cell-independent b cell response is responsible for ABC phenomenon induced by repeated injection of PEGylated liposomes. *Int. J. Pharm.* **2010**, *392*, 218−223.

(17) Koide, H.; Asai, T.; Hatanaka, K.; Urakami, T.; Ishii, T.; Kenjo, E.; Nishihara, M.; Yokoyama, M.; Ishida, T.; Kiwada, H.; Oku, N. Particle size-dependent triggering of accelerated blood clearance phenomenon. *Int. J. Pharm.* **2008**, *362*, 197−200.

(18) Abu Lila, A. S.; Kiwada, H.; Ishida, T. The accelerated blood clearance (ABC) phenomenon: clinical challenge and approaches to manage. *J. Controlled Release* **2013**, *172*, 38−47.

(19) Hara, E.; Makino, A.; Kurihara, K.; Sugai, M.; Shimizu, A.; Hara, I.; Ozeki, E.; Kimura, S. Evasion from accelerated blood clearance of nanocarrier named as "lactosome" induced by excessive administration of lactosome. *Biochim. Biophys. Acta* **2013**, *1830*, 4046−4052.

(20) Ishida, T.; Atobe, K.; Wang, X. Y.; Kiwada, H. Accelerated blood clearance of PEGylated liposomes upon repeated injections: effect of doxorubicin-encapsulation and high-dose first injection. *J. Controlled Release* **2006**, *115*, 251−258.

(21) Nomura, A.; Okayasu, K.; Ohno, K.; Fukuda, T.; Tsujii, Y. Lubrication mechanism of concentrated polymer brushes in solvents: effect of solvent quality and thereby swelling state. *Macromolecules* **2011**, *44*, 5013−5019.

(22) Tsujii, Y.; Ohno, K.; Yamamoto, S.; Goto, A.; Fukuda, T. Structure and properties of high-density polymer brushes prepared by surface-initiated living radical polymerization. *Adv. Polym. Sci.* **2006**, *197*, 1−45.

(23) Makino, A.; Hara, E.; Hara, I.; Ozeki, E.; Kimura, S. Size control of core-shell-type polymeric micelle with a nanometer precision. *Langmuir* **2014**, *30*, 669−674.

(24) Kaminskas, L. M.; McLeod, V. M.; Porter, C. J. H.; Boyd, B. J. Differences in colloidal structure of pegylated nanomaterials dictate the likelihood of accelerated blood clearance. *J. Pharm. Sci.* **2011**, *100*, 5069−5077.

(25) Ishihara, T.; Maeda, T.; Sakamoto, H.; Takasaki, N.; Shigyo, M.; Ishida, T.; Kiwada, H.; Mizushima, Y.; Mizushima, T. Evasion of the accelerated blood clearance phenomenon by coating of nanoparticles with various hydrophilic polymers. *Biomacromolecules* **2010**, *11*, 2700−2706.

(26) Ma, H. L.; Shiraishi, K.; Minowa, T.; Kawano, K.; Yokoyama, M.; Hattori, Y.; Maitani, Y. Accelerated blood clearance was not induced for a gadolinium-containing peg-poly(L-lysine)-based polymeric micelle in mice. *Pharm. Res.* **2010**, *27*, 296−302.

(27) Hara, E.; Ueda, M.; Kim, C. J.; Akira, M.; Hara, I.; Ozeki, E.; Kimura, S. Suppressive immune response of poly(sarcosine) chains in peptide-nanosheets in contrast to polymeric micelles. *J. Pept. Sci.* **2014**, DOI: 10.1002/psc.2655.